

RESEARCH ARTICLE

# Meniscus heterogeneity and 3D-printed strategies for engineering anisotropic meniscus

Ming-Ze Du<sup>†</sup>, Yun Dou<sup>†</sup>, Li-Ya Ai, Tong Su, Zhen Zhang, You-Rong Chen\*, Dong Jiang\*

Department of Sports Medicine, Peking University Third Hospital, Institute of Sports Medicine of Peking University, Beijing Key Laboratory of Sports Injuries, Beijing, 100191, China

(This article belongs to the *Special Issue: Advances in 3D bioprinting for regenerative medicine and drug screening*)

## Abstract

The meniscus is a fibrocartilaginous tissue of the knee joint that plays an important role in load transmission, shock absorption, joint stability maintenance, and contact stress reduction. Mild meniscal injuries can be treated with simple sutures, whereas severe injuries inevitably require meniscectomy. Meniscectomy destroys the mechanical microenvironment of the knee joint, leading to cartilage degeneration and osteoarthritis. Tissue engineering techniques, as a strategy with diverse sources and customizable and adjustable mechanical and biological properties, have emerged as promising approaches for the treatment of meniscal injuries and are represented by 3D printing. Notably, the heterogeneity of the meniscus, including its anatomical structure, cell phenotype, extracellular matrix, and biomechanical properties, is crucial for its normal function. Therefore, the construction of heterogeneous tissue-engineered menisci (TEM) has become a research hotspot in this field. In this review, we systematically summarize the heterogeneity of menisci and 3D-printed strategies for tissue-engineered anisotropic menisci. The manufacturing techniques, biomaterial combinations, surface functionalization, growth factors, and bioreactors related to 3D-printed strategies are introduced and a promising direction for the future research is proposed.

**Keywords:** Meniscus; Heterogeneity; Tissue engineering; 3D printing

<sup>†</sup> These authors contributed equally to this work

**\*Corresponding authors:**

Dong Jiang  
(bysyjiangdong@126.com)  
You-Rong Chen  
(chenyourong1990@pku.edu.cn)

**Citation:** Du MZ, Dou Y, Ai LY, 2023, Meniscus heterogeneity and 3D-printed strategies for engineering anisotropic meniscus. *Int J Bioprint*, 9(3): 693. <https://doi.org/10.18063/ijb.693>

**Received:** August 25, 2022

**Accepted:** November 12, 2022

**Published Online:** February 27, 2023

**Copyright:** © 2023 Author(s). This is an Open Access article distributed under the terms of the Creative Commons Attribution License, permitting distribution, and reproduction in any medium, provided the original work is properly cited.

**Publisher's Note:** Whioce Publishing remains neutral with regard to jurisdictional claims in published maps and institutional affiliations.

## 1. Introduction

The meniscus, an indispensable structure located in the knee joint, assumes the biofunctions of load transmission, shock absorption, joint lubrication, and proprioception<sup>[1-3]</sup>. Biologically, the intact meniscus stabilizes and coordinates the flexible knee joint by enlarging the contact area between the condyle femur and tibia plateau, as well as cushioning friction between cartilage<sup>[4-6]</sup>. Total meniscectomy<sup>[7]</sup>, reported in 1948, is generally recognized as the only feasible strategy to treat meniscal tears, which is one of the most common sports injuries<sup>[8]</sup>. Partial meniscectomy was then recommended as a substitute for total meniscectomy<sup>[9]</sup> for severe meniscal injury in 1982. Nonetheless, research has demonstrated that the femur and tibia would directly contact a smaller area with higher stress after meniscectomy<sup>[10]</sup>, leading to

a 2 – 7-fold higher risk of osteoarthritis<sup>[11]</sup>. Meanwhile, the remaining section of the meniscus was confirmed to suffer from increased compressive pressure, accelerating the degeneration of cartilage and ultimately osteoarthritis of the knee joint<sup>[12]</sup>. Therefore, attempts to maintain the integrity of the meniscus after injury have reached an overwhelming consensus. Disappointingly, with adequate vascularity in only 10 – 25% peripheral red-red zone, severe tears in the avascular white-white zone showed no potential for self-repair<sup>[13,14]</sup>. Allografts of meniscus substitutes, although effective, are clinically limited by scarce sources. Some products, although already clinically applied, such as CMI® and Actifit®, have a high failure rate of 30% due to a deficiency in blood supply after implantation, resulting in failure of regeneration and progression of articular cartilage lesions<sup>[15,16]</sup>. On this account, tissue-engineered meniscus (TEM) shows promising prospects as an ideal implant in meniscus repair<sup>[17-22]</sup>.

The meniscus is a semilunar fibrocartilaginous tissue characterized between the fiber and hyaline cartilage, which combines the properties of ligaments to withstand tensile forces and the properties of hyaline cartilage to withstand compressive and shear forces<sup>[23,24]</sup>. However, in contrast to homogeneous ligaments and cartilage, menisci show sophisticated heterogeneity in anatomy, cell phenotypes, extracellular matrix (ECM), and biomechanical properties<sup>[25,26]</sup>. This anisotropic structure enables knee joints to adapt to flexion and rotate with different strains at different angles, efficiently transmitting load and protecting articular cartilage from abrasion<sup>[27,28]</sup>. Accordingly, only a TEM with bionic heterogeneity can adequately function as a natural meniscus in the knee joint. To reconstruct the heterogeneity of the meniscus, scientists have attempted several three-dimensional (3D) printing methods, which have indicated inspiring outcomes both *in vitro* and *in vivo*. Therefore, we systemically reviewed the heterogeneity of the meniscus to obtain insights into the construction of TEM with more biomimetic properties (Figure 1). The databases of PubMed, Web of Science, and Embase were searched systematically to collect relevant reports published since January 1990. Original articles that involved anisotropic meniscus tissue engineered reconstruction were selected for analysis, in which articles related to 3D printing were included, and other strategies, *for example*, electrospinning, freeze-drying technique, *etc.*, were excluded from the study. In addition, after discussing the research status and progress of 3D printing heterogeneous TEM, references are also provided in this paper for future research. Different from previous reviews, the present review paper focuses on the meniscus heterogeneity and TEM strategies, especially from the

studies involving 3D printing technique, and provides the latest, detailed and comprehensive summary about 3D-printed anisotropic TEM.

## 2. Heterogeneity of meniscus

### 2.1. Anatomy and histology of meniscus

The meniscus is a pair of crescent-shaped structures placed inside the knee joint capsule, protecting the condyles of the femur and tibial plateau from direct contact. The hyaline cartilage, fibrocartilage, connective tissues, and composition of the meniscus vary in proportion to zones, species, and age<sup>[14,24]</sup>. Shaped at 8 – 10 weeks of pregnancy<sup>[29]</sup>, the medial and lateral menisci are not macroscopically identical. The medial meniscus is C-shaped, approximately 40 – 45 mm in length and 27 mm in width, covering 51 – 74% of the medial joint surface<sup>[23,30,31]</sup>. The lateral meniscus, shorter but larger than the medial meniscus, is O-shaped, 32 – 35 mm in length, and covers 75 – 93% of the joint surface<sup>[30,31]</sup>. The posterior horn of the lateral meniscus is attached to the intercondylar region of the tibia, neighboring the posterior horn of the medial meniscus<sup>[32]</sup>. The meniscotibial ligaments, the capsule thickening between the apex of the fibular head, and the inferolateral portion of the lateral meniscus fix the meniscus to the tibia<sup>[33,34]</sup>. The meniscus is composed of the ligament of Humphrey anterior to the posterior cruciate ligament and the ligament of Wrisberg posterior to it, attaching the meniscus with the femur condyle<sup>[35]</sup>. Moreover, the transverse ligament moves between the anterior horns of the bilateral menisci, connecting them as a functional unit<sup>[35]</sup>.

Blood supply to the meniscus originates from the peripheral perimeniscal capillary plexus, which originates from the branches of the medial inferior, lateral inferior, and middle geniculate arteries<sup>[36]</sup>. The meniscoligamentous complex is derived from the intermediate layer of mesenchymal tissue. From the embryo to the early postpartum period, the meniscus is highly cellular and vascularized, with extensive blood supply to the whole tissue<sup>[13,32]</sup>. Under gradual regression of vessels, only 10 – 30% of the meniscus in the outer region is vascularized at age 10, while vessels and nerves exist in only 10 – 25% of the peripheral meniscus in adults<sup>[14,37]</sup>. Due to avascularity in the inner portion of adults, tears are difficult to self-repair. Several therapeutic approaches have been developed to repair such non-healing injuries through angiogenesis, including vascular endothelial growth factor (VEGF), connective tissue growth factor (CTGF), and hepatocyte growth factor (HGF), which are administered directly into the knee joint or used as an auxiliary method for bioengineering<sup>[38]</sup>. Meanwhile, a decrease in cells and

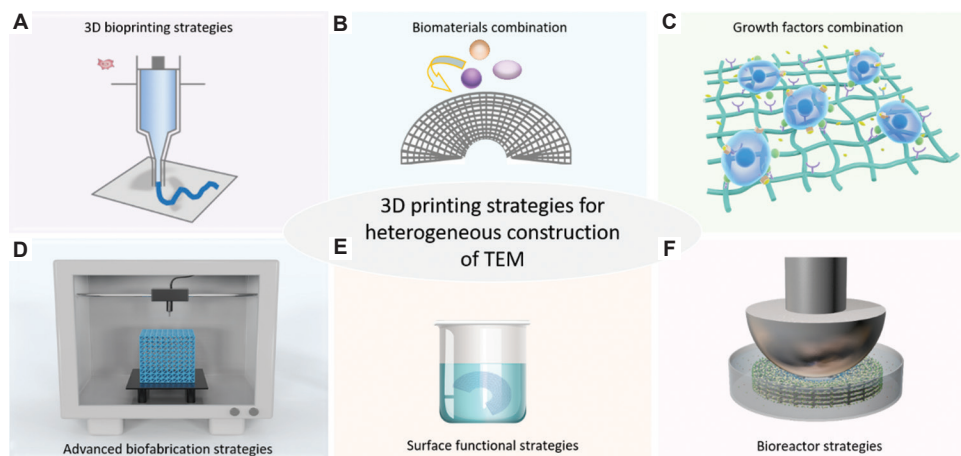


**Figure 1.** Schematic of 3D printing strategies for heterogeneous construction of tissue-engineered menisci (TEM). (A) 3D bioprinting applied for heterogeneous TEM. (B) Combined biomaterials applied for 3D-printed heterogeneous TEM. (C) Growth factors applied in 3D printing of heterogeneous TEM. (D) Advanced and biomimetic biofabrication strategies applied for 3D-printed heterogeneous scaffolds. (E) Surface functional strategies applied for heterogeneous TEM. (F) Bioreactors applied for 3D-printed heterogeneous scaffolds.

an increase in circumferential fibers can be observed due to movement and stress loading of the knee joint<sup>[32,39]</sup>.

Nerves follow the same distribution as vessels. The recurrent peroneal branch of the common peroneal nerve dominates the lateral capsule, as well as the peripheral meniscus<sup>[24]</sup>. In contrast, the inner white-white zone is non-innervated. Mechanoreceptors and nociceptors can be found in the meniscus, but are not as sensitive and accurate as in the synovium and joint capsule<sup>[40]</sup>.

## 2.2. Biological heterogeneity of meniscus

Constituted by the hydrophilic ECM, the meniscus is rich in water (72%) and collagen (22%), with only a few cells. Most of the water is retained in the proteoglycans. As an avascular structure, the meniscus of the white-white zone is nourished by synovial fluid. In terms of high water volume, large hydraulic pressures are required for expedited metabolism<sup>[24]</sup>. Collagens (75% of dry weight) make up the majority of organic matter in the meniscus, followed by proteoglycans (17%), DNA (2%), elastin (<1%), and adhesion glycoproteins (<1%). The proportion of components may vary slightly with age, lesions, and other pathological states<sup>[5,41-44]</sup>. The heterogeneity of vascularity, cell type, and ECM components facilitates the complex biological functions of the meniscus.

As mentioned above, vessels and nerves exist only in the outer third of the synovial margin of the meniscus. Therefore, the meniscus can be divided into three zones: The outer third, red-red zone; the inner third, white-white zone; and the transitional third, red-white zone between the former two (Figure 2). Unlike the adequate blood supply and nerve that can be found in the red-red zone,

the white-white zone is avascular and non-innervated, with metabolism and nutrition relying on synovial fluid. Due to the tardiness of transportation by synovial fluid, lesions in the white-white zone can hardly repair itself, which accounts mainly for clinical failure of self-healing after meniscus tear. The red-white zone, a transitional region between the red and white zones, is characterized by both<sup>[13,21]</sup>.

Cells in the meniscus, known as fibrochondrocytes, including fibroblast-like and chondrocyte-like cells, also show high heterogeneity<sup>[24,45,46]</sup> (Figure 2). Fusiform fibroblast-like cells appear more in the outer zone, whereas oval chondrocyte-like cells can be distinguished in the inner zone<sup>[47,48]</sup>. This variation in morphology seems to result from the discrepancy in the force that the meniscus withstands in the different zones. In the peripheral region, fibrochondrocytes are stretched to better adapt to circumferential tension, while compressive forces maintain the spherical shape of the cells<sup>[49]</sup>. According to their shape and secreted ECM, cells are classified into chondrocytes, fibroblasts, and intermediate cells with both characteristics<sup>[48]</sup>.

Because of the heterogeneity in cell type and applied force, ECM also exhibits heterogeneity due to its diverse subtypes and anisotropic alignment. Type I collagen (COL-1) predominates in the peripheral region, whereas the inner zone is mainly composed of glycosaminoglycan (GAG) and Type II collagen (COL-2)<sup>[1,50-52]</sup>. Collagens align randomly at the superficial layer, while circumferentially forming bundles in the deeper layer with a few radially interwoven in the meniscus<sup>[23,53]</sup>. Elastin, which is low in volume (0.6%), is another fibrillar component with unclear biochemical essentiality<sup>[21]</sup>. Adhesion glycoproteins, elastin

and GAG, bundling and networking with collagens provide a dedicated microstructure for the meniscus with excellent biomechanical properties<sup>[54]</sup>.

### 2.3. Biomechanical heterogeneity of meniscus

Compressing forces, approximately 3–4 folds of body weight in daily activities, are transmitted along the femur condyles and tibial plateau<sup>[28,55]</sup>. The meniscus withstands 50–70% of the axial stress, thereby protecting articular cartilage from early degeneration<sup>[56-59]</sup>. Apart from compression, the meniscus also withstands diverse types of forces such as shear and tension. Its prominent biomechanical properties make the meniscus an indispensable structure in load bearing, force transmission, shock absorption, and joint lubrication (Figure 3).

The meniscus displays an intricate mechanical microenvironment, undergoing morphological changes

such as flexion and rotation as the knee joint moves<sup>[60]</sup>. An early study investigated the anisotropic biomechanics in the circumferential, radial, and axial directions, and found that axial stiffness is significantly greater than both circumferential and radial stiffness<sup>[27]</sup>. As an elastic gasket in the knee joint, it showed a low average radial or circumferential stretch (<1%) but 12% of axial strain<sup>[61]</sup>. In flexion, up to 90% of compression is transmitted through the lateral meniscus. Researchers zoned the meniscus into two regions with different microstructures through microscopy and scanning electron microscopy observations: The inner two-thirds and remaining outer one-third. Such a specific structure fundamentally accounts for the specific function of the meniscus: The inner zone bearing compression and the outer zone withstanding tension. This transition, which varies with region, represents an apparent aspect of biomechanical heterogeneity that is important for

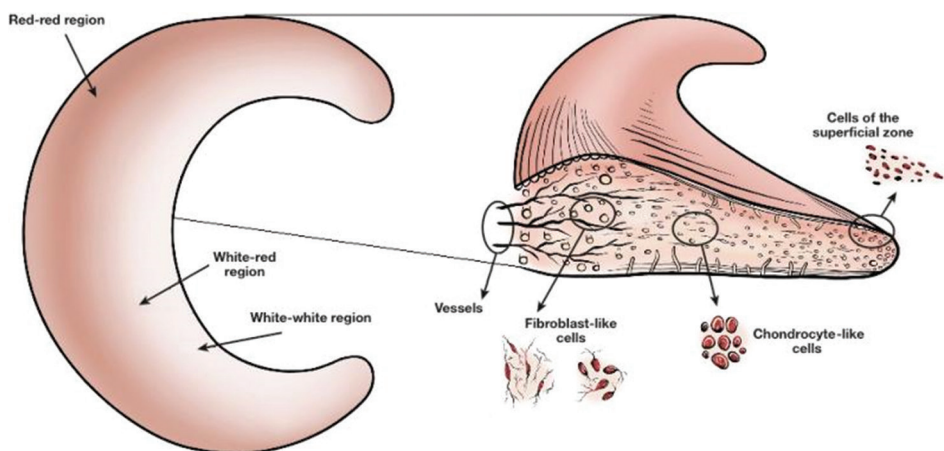


**Figure 2.** Schematic diagram of the structure of heterogeneous meniscus. Left: Although fully vascularized after born, vessels in the meniscus are under gradual degeneration, remaining merely in the red-red zone in adults. Right: Cells in the outer, vascularized red-red zone are in fusiform shape similar to fibroblasts, while oval cells are found similar to chondrocytes in red-white zone and white-white zone. Furthermore, there are some small and round cells discovered on the surface of meniscus. Reprinted from *Biomaterials*, 32, Makris EA, Hadidi P, Athanasiou KA, The knee meniscus: Structure-function, pathophysiology, current repair techniques, and prospects for regeneration, 7411–7431., Copyright (2011), with permission from Elsevier.

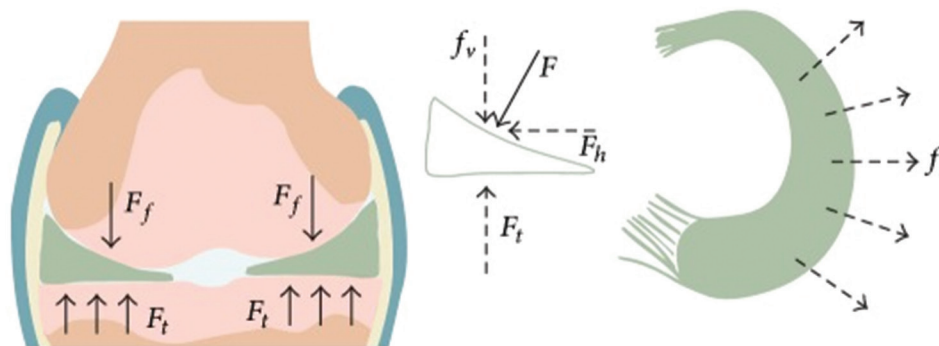


**Figure 3.** Force analysis of meniscus. Wedge-shaped meniscus adapts well to femur condyles and tibia plateau. Vertical loading ( $F$ ) and horizontal force ( $F_h$ ) come from compressing the femur.  $F_r$  radially compresses the meniscus, which can be offset through ligaments anchored at the anterior and posterior horn. Therefore, axial force can be translated into circumferential tension (from ref. [72] licensed under Creative Commons Attribution license).

joint stabilization and cartilage protection<sup>[62,63]</sup>. In a study performed by Moyer *et al.*, the medial-posterior region was confirmed to have the lowest elastic friction value through indentation, which corresponded to the low GAG intensity<sup>[64]</sup>. Gonzales-leon *et al.* regionally studied meniscus biomechanics in a minipig model that is biologically similar to a human meniscus. In their research, the radial Young's modulus was not significantly different between bilateral menisci but was remarkably higher in the anterior region than in the posterior region, which may explain the relative susceptibility to longitudinal tears of the posterior meniscus. In addition, the posterior region was found to have the highest tensile strength in the medial meniscus, whereas no significant difference was found in the lateral meniscus<sup>[65]</sup>.

Furthermore, considering that circumferential fibers predominate in the meniscus, biomechanical heterogeneity is also exhibited by tensile strength. Research has shown that the circumferential tensile modulus, 75 – 150 MPa, is approximately 10 times higher than the radial tensile modulus<sup>[42,66]</sup>. Excellent tensile strength buffers the loading circumferentially applied to the meniscus and radially resists outward dislocation.

The fluid phase is also worthy of attention as another aspect of anisotropy. The hydraulic permeability ranges from  $10^{-15}$  to  $10^{-14}$  m<sup>4</sup>/N s for confined compression<sup>[67]</sup> and  $10^{-15}$  to  $10^{-15}$  m<sup>4</sup>/N s for indentation<sup>[68]</sup>. This hydraulic permeability is of great importance in high levels of load bearing and is also influenced by the fiber network. Heterogeneity is also found circumferentially and radially between the pars intermedia and posterior horn in the fluid phase<sup>[69]</sup>. Biomechanical heterogeneity plays an essential role in functionalizing the meniscus and stabilizing the knee joint. This biomechanical heterogeneity results from the anisotropic alignment of collagen fibers as well as other ECM components. In return, the variant biomechanical microenvironment also influences cells and the ECM both morphologically and biochemically. A 5% of biaxial tensile strain at 0.5 Hz increased protein synthesis but did not influence the secretion of proteoglycan<sup>[70]</sup>, while uniaxial tensile strain promoted COL-1 expression in inner meniscal cells but not in outer cells<sup>[71]</sup>. The precise biomechanical properties as well as the interaction between cells and the ECM are not fully understood, requiring more research on this topic. The heterogeneity of the meniscus is summarized in Table 1.

### 3. 3D printing of heterogeneous TEM

As discussed above, the meniscus shows high heterogeneity in cell type, ECM, and biomechanisms<sup>[47,54]</sup>. Therefore,

biomimetic reconstruction of heterogeneous meniscus is inevitable in TEM.

3D printing, a widely used technique in medical fields with the advantages of high efficiency and customizability, provides a novel strategy to construct TEM<sup>[73]</sup>. 3D-printed TEM has achieved eye-catching results. In this review, we systematically summarize the strategies utilized to fabricate heterogeneous 3D-printed TEM, focusing on the manufacturing technique, biomaterial combination, 3D bioprinting, surface functionalization, growth factors, and bioreactors.

#### 3.1. Advanced and biomimetic biofabrication strategies applied for heterogeneous 3D-printed scaffolds

Diverse biostructures exist in the natural world that perform their own duties. For instance, the claws of lobsters, rich in well-organized layers of chitosan with anisotropic Bouligand structures inlaid, not only exhibit powerful mechanisms but also exhibit high energy dissipation and impact resistance because of the long-term evolution of the structure<sup>[74]</sup> (Figure 4). This reminds us that a specific structure is required to realize the optimum microenvironment, which is also an enlightenment to fabricate TEM with a highly heterogeneous structure.

To realize specific biomechanical heterogeneity in the meniscus through structural design, Yang *et al.* combined a 3D printing technique with carbon nanotubes (CNTs)<sup>[74]</sup>. CNTs have great potential in fields such as nanomaterials, due to their excellent mechanical properties. In their research, with the assistance of electrically assisted additive manufacturing/3D printing technology, a reinforcement architecture was fabricated with anisotropic layers of aligned surface-modified multi-walled carbon nanotubes (MWCNT-S). Mechanical testing demonstrated that the augmented circumferential tensile strength improved energy dissipation and compression resistance regulated through rotation angles, providing a novel method to realize the biomimetic properties of TEM. In addition, Bahcecioglu *et al.* designed a poly( $\epsilon$ -caprolactone) (PCL)/hydrogel composite scaffold that mimics the structural organization, biochemistry, and anatomy of the meniscus<sup>[75]</sup>. The compression strength ( $380 \pm 40$  kPa) and tensile modulus ( $18.2 \pm 0.9$  MPa) were significantly increased by the circumferential collagen strands. Meanwhile, the proliferation and migration of fibrochondrocytes are also promoted by circumferentially aligned PCL fibers. Such research has shown the importance of biomimetic design in tissue engineering, particularly for tissues with mechanical heterogeneity, such as menisci.

Table 1. Heterogeneity of the meniscus

Aspects	Contents	Relevant manifestation	Reference	
Anatomy heterogeneity	Shape	Length: 40.5 – 45.5 mm (medial meniscus), 32.4 – 35.7 mm (lateral meniscus)	[30,31]	
		Width: 27 mm (medial meniscus), 26.6 – 29.3 mm (lateral meniscus)		
		Shape: C-shaped (medial meniscus), O-shaped (lateral meniscus)		
	Vessel, nerve and lymph	Red-red zone: the outer 10 – 25% of the meniscus which is penetrated with vessels, nerves and lymph	[13,21]	
Red-white zone: the transitioning area		[2,3]		
White-white zone: the inner 1/3 of the meniscus which is avascular, aneural and alymphatic				
Biological heterogeneity	Extracellular matrix components	In general: Water (72%), collagens (22%), proteoglycans (1%), DNA (2%), elastin (<1%) and adhesion glycoproteins (<1%). Proportion varies with age, lesions and pathological states.	[24,41-44]	
	Collagen	Red-red zone: Collagen I (80% of dry weight), Collagen II, III, IV, VI, XVIII (<1% of dry weight)	[50-52]	
		White-white Zone: Collagen I (40% of dry weight), Collagen II (60% of dry weight)		
	Cell phenotype	Fusiform fibroblast-like cells in the outer zone while oval chondrocyte-like cells in the inner zone with respective biological actions.	[47,48]	
Biomechanical Heterogeneity	Compression	At low strain:	Circumferential: 10 MPa	[27]
			Radial: 13 MPa	
			Axial: 19 MPa	
		At high strain:	Circumferential: 288 MPa	
			Radial: 287 MPa	
			Axial: 299 MPa	
		(Axial stiffness is significantly greater than both circumferential and radial stiffness)		
		Inner zone bears compression while outer zone withstands tension.	[62,63]	
	Tension	Circumferential	Medial anterior: 99.4 MPa	[42,66]
			Medial center: 107.9 MPa	
Medial posterior: 114.1 MPa				
Lateral anterior: 99.8 MPa				
Lateral center: 78.4 MPa				
Lateral posterior: 116.2 MPa				
Radial		Medial anterior: 10.5 MPa		
		Medial center: 7.6 MPa		
		Medial posterior: 2.5 MPa		
		Lateral anterior: 10.9 MPa		
	Lateral center: 10.3 MPa			
	Lateral posterior: 8.5 MPa			
	Circumferential tensile modulus is 10-fold higher than radial modulus.			
	Radial Young's modulus is remarkably higher in the anterior region than posterior region.	[65]		
	The highest tensile strength in medial meniscus appears in the posterior region.	[65]		
Hydromechanics	Hydraulic permeability ranges from $10^{-15}$ to $10^{-14}$ m <sup>4</sup> /N s for confined compression and $10^{-17}$ – $10^{-15}$ m <sup>4</sup> /N s for indentation.	[68]		
	Heterogeneity is also found circumferentially and radially between pars intermedia and posterior horn in fluid phase.	[69]		

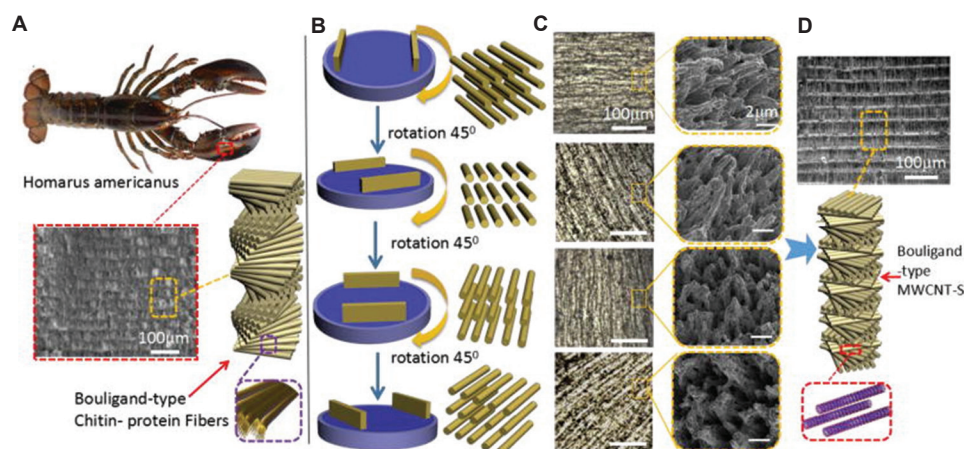


**Figure 4.** Biomimetic structure of MWCNT-S constructed by electrically assisted 3D printing. (A) Schematic diagram of the American lobster and the microstructure of lobster claws made from chitin protein fibers. (B) The carbon nanotubes can be arranged in different directions by adjusting the rotating electrode. (C) Surface microscope images and tomographic SEM images of different arrays of MWCNT-S corresponding to (B). (D) Schematic diagram of the layered biological ligand MWCNT-S fabricated by electrically assisted nanocomposite 3D printing (from ref. [74] licensed under Creative Commons Attribution license).

The microvascular system widely exists in most tissues of the human body and plays an important role in metabolism, nutrition supply, and gas exchange<sup>[76]</sup>. Similarly, there is heterogeneity in the spatial distribution of blood vessels in the meniscus, and the injured meniscus is often difficult to repair itself because in adulthood, only the lateral 1/3 of the meniscus has a blood supply<sup>[21]</sup>. Therefore, in terms of biomanufacturing, simulating the heterogeneous vascular distribution of the meniscus through a multiplex biofabrication strategy can provide the necessary nutrition for meniscus regeneration. Multi-biomaterial 3D printing strategies have been used to reconstruct heterogeneous vascular distributions. Margo *et al.* developed a proangiogenic and antiangiogenic bioink containing endothelial cells (ECs), supplemented by bioactive matrix-derived microfibrils (MF) made of Type I collagen sponge (COL-1) and cartilage acellular extracellular matrix (CdECM), which can promote or inhibit capillary network regeneration for the biological manufacture of tissues with anisotropic microvascular distribution<sup>[77]</sup>.

Biochemical heterogeneity is another important characteristic of menisci. Research has shown that the microstructures of bioactive materials can influence the activity and differentiation of exogenous and endogenous seed cells<sup>[78,79]</sup>, among which the mean pore size of the scaffold can directly regulate the interaction between the cells and matrix effectively. Zhang *et al.* demonstrated that the mean pore size of scaffolds plays a vital role in the biological activity of seed cells<sup>[80]</sup>. They constructed three scaffolds with different pore size (215 μm, 320 μm, 515 μm), confirmed a positive correlation between the

colonization area of MSCs and the surface area per unit volume (SA/V). In addition, Col-2 deposition was positively correlated with SA/V. Gradient structure is also an important concept in regenerative medicine. Similarly, a gradient change was observed in the meniscus from the inner hyaline chondrocytes to the outer fibrochondrocytes. Andrea *et al.* designed a novel hierarchical scaffold with different pore sizes and illustrated that pore size is a non-negligible factor in stem cell differentiation. They further revealed that smaller pores were more beneficial for chondrogenic differentiation<sup>[81]</sup>. Therefore, a 3D-printed scaffold with a pore size gradient is effective in generating medicine, particularly in tissues, such as the meniscus and bone.

The main challenges of heterogeneous TEM include compatible anatomical shape, excellent mechanical properties, and microstructure that can mimic the structure of ECM to play a key role in the meniscus in knee kinematics and homeostasis<sup>[82]</sup>. Other studies have also reported bionic biological strategies for constructing heterogeneous TEM. Thiago *et al.* developed a 3D-printed meniscus scaffold with a customized macro size and microstructure, which consisted of an ECM fiber structure based on a natural meniscus. A mechanical compression test showed that the structural integrity and shape fidelity of the scaffold were enhanced by the aligned nanofiber layers between the hydrogel layers<sup>[83]</sup>. Ibrahim *et al.* proposed a 3D-printed PCL and porous silk fibroin cage (EIC) scaffold for meniscus tissue engineering, and the EIC scaffold demonstrated better interconnection, mechanical properties, cell adhesion, and proliferation ability<sup>[84]</sup>.

In summary, the key requirement of biofabrication strategies applied for heterogeneous 3D-printed TEM was to mimic the natural meniscus microstructure using advanced processing technique, so as to lay foundation for the functional meniscus reconstruction. So far, significant progress has been made in the preparation of heterogeneous TEM by changing the manufacturing process. It has the advantages of being controllable and not introducing other exogenous components. However, it is still a challenge to construct biomimetic meniscus grafts with both mechanical and biochemical heterogeneity, which requires more in-depth research.

### 3.2. Combined biomaterials applied for 3D-printed heterogeneous TEM

Considering the spatially anisotropic distribution of cells and ECM in the meniscus, several strategies have been attempted, such as the combination of different types of biomaterials to endow their respective advantages in appropriate regions, which is also a promising method<sup>[85]</sup>. The previous research has inspired the feasibility of combining multiple biomaterials to mimic biological menisci.

For instance, synthetic materials combined with hydrogels in specific proportions are prone to exhibit biological heterogeneity. Bahcecioglu *et al.* anatomically constructed a 3D-printed PCL scaffold with cast cell-loaded gelatin methacrylate (GelMA) in the periphery and GelMA-Ag in the inner region. *In vivo* experiments showed a significant increase in COL-1 deposition in the outer region, and chondrogenic differentiation of stem cells was promoted in the inner region<sup>[86]</sup>. Bahcecioglu *et al.* also demonstrated the biological reaction of stem cells in their previous research<sup>[75]</sup>. Romanazzo *et al.* demonstrated that alginate functionalized with peripheral meniscus ECM and promoted fibroblast differentiation of adipose-derived mesenchymal stem cells (MSCs) free from growth factors, while functionalizing the alginate with meniscus ECM from the inner margin induced chondrogenic differentiation with increased secretion of COL-2 and mucopolysaccharide sulfate. This composite hydrogel, when manufactured into bioink, showed great potential for constructing 3D-printed heterogeneous TEM<sup>[87]</sup>.

Microspheres encapsulating bioactive materials are favored as a promising approach to highlight anisotropic cell type and ECM deposition. Hao *et al.* 3D-printed a composite PCL/hydrogel scaffold dual-loaded with platelet-derived growth factor-BB (PDGF-BB) and the chondrogenic molecule kartogenin (KGN). They successfully achieved heterogeneity, with the migration of endogenous progenitor/stem cells (ESPCs) promoted

by PDGF-BB and chondrogenic differentiation induced by KGN<sup>[88]</sup> (Figure 5). They also proposed a 3D-printed PCL/MECM/KGN composite scaffold in which polylactic-co-glycolic acid (PLGA) microspheres encapsulated with KGN were used as a drug delivery system. The synergistic effect of sustained release of MECM and KGN endows the PCL/MECM-KGN microsphere scaffold with excellent cytocompatibility and chondrogenic activity<sup>[89]</sup>.

In tissue engineering, it is necessary to regulate inflammation in the receptor, such as by regulating the recruitment of leukocytes and the subsequent inflammatory process through drug delivery strategies<sup>[90,91]</sup>. Xu *et al.* prepared a 3D-printed polylactone/4 arm poly (ethylene glycol) hydrogel (PCL@ tetra-PEG) composite scaffold with anti-inflammatory and anti-oxidation effects, which was coated with the Ac2-26 peptide, demonstrating anti-inflammatory and anti-oxidation effects on regulating the complex microenvironment and promoting tissue regeneration<sup>[92]</sup> (Figure 6).

Silk fibroin (SF) is a natural high polymer fibrin extracted from silk that is extensively involved in tissue engineering because of its excellent biocompatibility, biomechanism, physiochemical properties, outstanding toughness, gas permeability, and release controllability<sup>[93,94]</sup>. A harmonious balance of biomechanical modulus and degradability can be achieved by combining SF and PCL, exhibiting great potential for mimicking biological menisci. In addition, SF sponges exhibit low surface shear and good elasticity, making them remarkable for load absorption and cartilage protection. Li *et al.* combined a synovium-derived MSC affinity peptide, LTHPRWP (L7), with a 3D-printed SF/PCL scaffold. This elaborately designed scaffold improved MSC proliferation, differentiation, and ECM secretion. Twenty-four weeks after implantation, the SF/PCL-L7 biomimetic meniscus acted similar to the natural meniscus, showing advantages in biomechanical properties, biological function, meniscus regeneration, and articular cartilage protection<sup>[95]</sup>. Pillai *et al.* proposed a multi-component composite 3D scaffold structure composed of SF and polyvinyl alcohol (PVA) with biomimetic enhancement and biomolecular functionalization for TEM. In addition, autoclaved eggshell membrane (AESM) powder was used to enhance the biomechanical properties of the scaffold<sup>[96]</sup>.

In addition, decellularized tissue-derived ECM, as a naturally extracted biomaterial, has shown tremendous potential in TEM. Decellularized extracellular matrix (DECM) not only maintains the biochemical properties of the microstructure, facilitating cell proliferation, but also regulates stem cell differentiation, specifically through growth factors<sup>[97,98]</sup>. DECM products are widely used as substitutes in regenerative medicine, such as



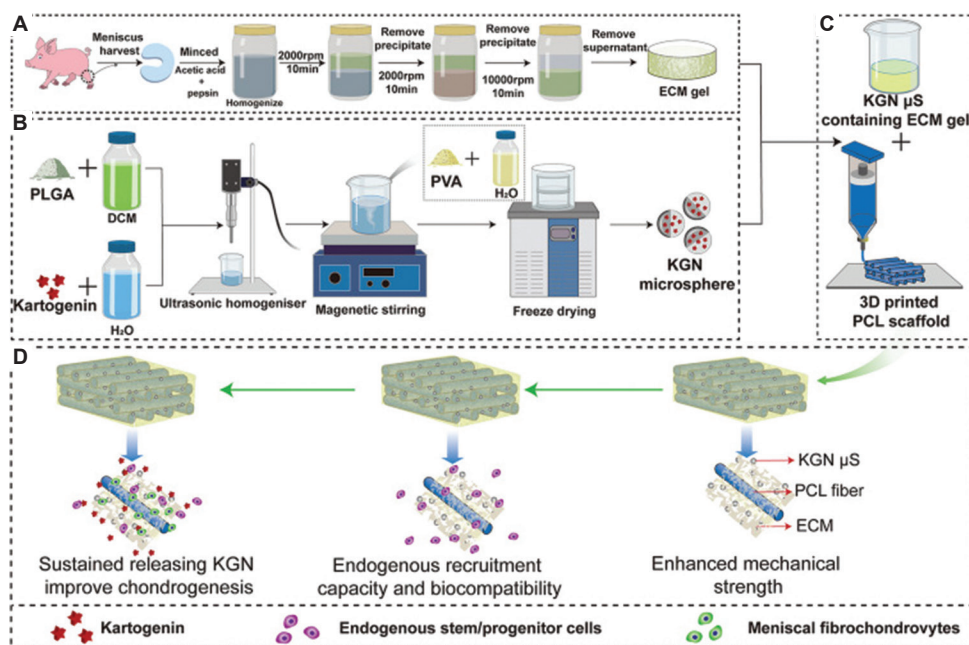


Figure 5. Schematic representation of the preparation process of the scaffolds (from ref. [88] licensed under Creative Commons Attribution license).

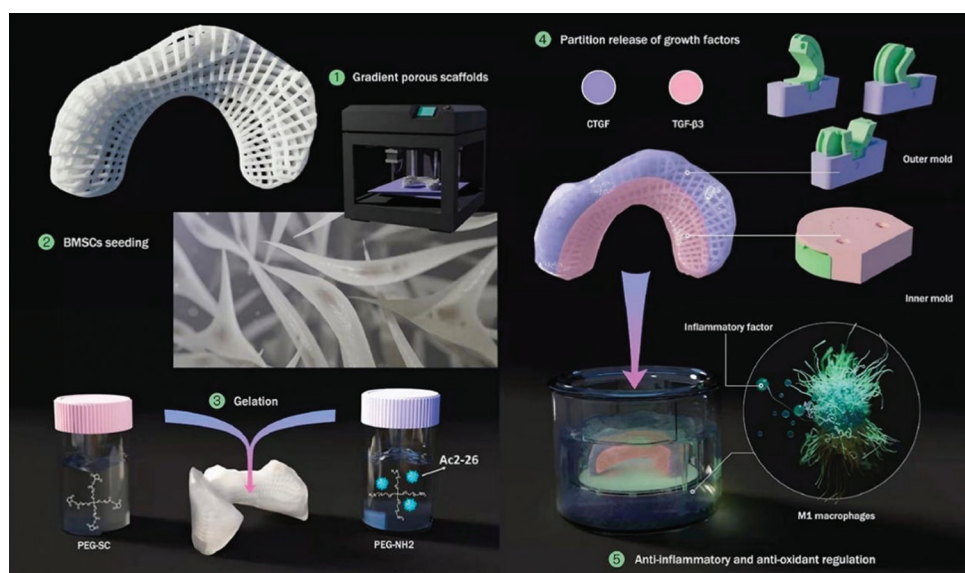


Figure 6. Schematic illustration of the whole study (from ref. [92] licensed under Creative Commons Attribution license).

skin, bladder, intestinal submucosa, pericardium, and heart valve, some of which are clinically applied<sup>[99-101]</sup>. Some studies have focused on the biocompatibility and potential of meniscus regeneration of decellularized meniscus extracellular matrix (DMECM)<sup>[99,102]</sup>. DMECM can be fabricated in the form of scaffolds, microspheres, bioinks, and hydrogels<sup>[99,103-106]</sup>. Guo *et al.* combined a PCL scaffold and DMECM with the assistance of a 3D printing technique to construct a biomimetic acellular DMECM scaffold. This dual-phase decellularized scaffold

demonstrated good biocompatibility and biomechanical properties, further accelerating meniscus regeneration and delaying osteoarthritis<sup>[107]</sup>. Cha *et al.* applied a cell-loaded DMECM bioink and polyurethane (PU)-PCL mixture for 3D-printed TEM, showing high controllability and long-lasting structural integrity. DMECM establishes a biomimetic microenvironment for stem cells, facilitating proliferation, and fibrochondrogenic differentiation<sup>[108]</sup>. In addition, to display its heterogeneity, some researchers have tried to extract DMECM from both the inner and

outer regions of the meniscus, revealing that DMECM derived from different regions functioned differently in bioaction<sup>[101,109]</sup>. In summary, 3D printing combined with DMECM bioink is a remarkable strategy for establishing the heterogeneity of the TEM microenvironment. Despite the progress of DMECM in meniscus regeneration, the specific components and properties of DMECM in different zones are still unclear. Furthermore, it is still a great challenge to gradually transmit from the inner to the outer zones of TEM, similar to the natural one.

### 3.3. 3D bioprinting applied for heterogeneous TEM

3D bioprinting is one of the most promising technologies for manufacturing biomimetic structures of heterogeneous tissues and organs<sup>[110]</sup>. 3D bioprinting technology has been used to manufacture clinically relevant patient-specific complex structures to achieve clinical requirements, such as menisci<sup>[111,112]</sup>. As a prospective therapeutic approach, functional substitutes can be successfully generated by coordinating appropriate cell sources and biomaterials through cell-based 3D bioprinting<sup>[113]</sup>.

Lan *et al.* synthesized bioink by combining human meniscus fibrochondrocytes (hMFC) from partial meniscectomy with cellulose nanofiber alginate hydrogel (TCNF/ALG). The results showed that the expression of COL2A1 in the TCNF/ALG scaffold was significantly increased, indicating an internal meniscus phenotype<sup>[113]</sup>. Costa *et al.* developed a highly elastic hybrid structure for fibrocartilage regeneration by printing a gellan/fibrinogen (GG/FB) composite bioink and silk fibroin methacrylate (Sil-MA) bioink containing cells in a staggered cross-hatch pattern. This bioprinted mechanically reinforced hybrid structure provides a versatile and promising alternative to the production of advanced fibrocartilage tissue<sup>[114]</sup>. Based on a multi-layer bionic strategy, Jian *et al.* optimized the preparation of meniscus-derived bioink and GelMA/meniscus extracellular matrix (MECM) to simultaneously consider printability and cell compatibility at the same time. The results of cell viability, mechanics, biodegradation, and tissue formation *in vivo* showed that the scaffold presented sufficient feasibility and functionality<sup>[115]</sup>. Sun *et al.* constructed a PCL scaffold using a 3D bioprinting technique combined with hydrogels loaded with PLGA microspheres and stem cells to release transforming growth factor- $\beta$ 3 (TGF- $\beta$ 3) and CTGF. TGF- $\beta$ 3, in the inner two-thirds region, is a hyaline chondrogenic inducer, and CTGF, together with Mg<sup>2+</sup> in the outer one-third region, promotes angiogenesis and the fibrochondrocyte phenotype. *In vivo* experiments illustrated that the 3D-printed TEM reestablished the heterogeneity similar to the natural meniscus as well as angiogenesis, significantly improved knee joint function,

and prevented secondary articular degeneration at the same time<sup>[103]</sup>.

### 3.4. Surface functional strategies applied for heterogeneous TEM

Meniscus reconstruction remains a challenge in clinical treatment due to its poor regenerative ability and structural complexity. 3D printing of polymer scaffolds is supposed to accurately construct complex tissue structures, but the polymer scaffolds usually lack sufficient biological activity to effectively promote regeneration. Scientists have tried to functionalize the surface of the scaffold to improve its biological activity to promote cell adhesion and proliferation enhancement, as well as the ability of chondrogenic/fibrochondrogenic capacity to construct a regional heterogeneity bionic to the natural meniscus.

Gupta *et al.* manufactured a 3D printing scaffold, composed of the overall structure of a carbohydrate-based self-healing interpenetrating network (IPN) based on a hydrogel. The surface of 3D printed PLA scaffold was functionalized and embedded with a self-healing IPN hydrogel for interface bonding, showing good biocompatibility and promoting meniscal tissue regeneration *in vivo*<sup>[116]</sup>. Deng *et al.* manufactured a customized polyurethane (PU) porous scaffold simulating a natural meniscus using low-temperature printing technology. To enhance the bioactivity of scaffolds cultured with human mesenchymal stem cells (hMSCs), surface modification of scaffolds by physical absorption of collagen I and fibronectin (FN) was detected by live/dead cell staining and cell viability assays. The results showed that fibronectin coating was superior to collagen I coating in promoting various stem cell functions, and fibronectin was conducive to the formation of cartilage on scaffolds<sup>[117]</sup>. Scaffolds derived from PCL have been widely explored in the field of TEM because of their biological safety and biomechanical properties. However, the poor intrinsic hydrophobicity of PCL hinders its widespread application in scaffold-assisted tissue regeneration. Zhou *et al.* developed a simple three-dimensional (3D) PCL scaffold surface modification strategy to increase the hydrophilicity and roughness of the scaffold surface through a simple sodium hydroxide (NaOH) solution immersion treatment. The results showed that hydrophilic modification can improve the proliferation and adhesion of cells on scaffolds<sup>[118]</sup>.

### 3.5. Bioreactors applied for 3D-printed heterogeneous scaffolds

Bioreactors combined with cell-loaded 3D-printed scaffolds are recognized as an effective approach for realizing meniscus heterogeneity. Computer models of bioreactor

Table 2. 3D printing strategies of heterogeneous TEM

Strategies combined with 3D printing	Materials	Methods and process	<i>In vitro</i> / <i>In vivo</i>	Biological effect of heterogeneity reconstruction	References
Advanced and biomimetic biofabrication strategies	MWCNTs	Reinforcement architecture with anisotropic layers of aligned surface modified MWCNTs.	<i>In vitro</i>	High energy dissipation and compressive modulus regulated by the strand ankle	[74]
	PCL/hydrogel	Fibers were circumferentially aligned that would mimic the structural organization, biochemistry and anatomy of meniscus.	<i>In vitro</i>	Good mechanical property and cytocompatibility induced by the circumferentially aligned PCL/hydrogel fibers.	[75]
	ECs/MF/COL-1/CdECM	Promote or inhibit angiogenesis through the biological manufacture of anisotropic biomaterials.	<i>In vitro</i>	Anisotropic distribution of blood vessels.	[77]
	PCL	The scaffold was designed into different mean pore size (215 $\mu\text{m}$ , 320 $\mu\text{m}$ , 515 $\mu\text{m}$ ).	<i>In vitro</i> and <i>in vivo</i>	The scaffold with 215 $\mu\text{m}$ mean pore size presented superior regeneration effect both <i>in vitro</i> and <i>in vivo</i> .	[80]
	PCL	A novel hierarchical scaffold was designed with different pore size.	<i>In vitro</i>	Smaller pores were supposed to be more beneficial for chondrogenic differentiation.	[81]
	Hydrogel	Aligned nanofiber layers.	<i>In vitro</i>	The structural integrity and shape fidelity of the scaffold were enhanced by aligned nanofiber layers between the hydrogel layers.	[83]
	EIC	Cage-shaped scaffold.	<i>In vitro</i>	EIC scaffold demonstrated better interconnection, mechanical properties and cell adhesion and proliferation ability.	[84]
Biomaterials	PCL/GelMA	Cell-loaded GelMA was incubated in the periphery and GelMA-Ag in the inner region.	<i>In vitro</i>	COL-1 deposition was significantly increased in the outer zone, and chondrogenic differentiation of stem cells was found in the inner zone.	[86]
	Alginate/ECM	The scaffold was based on alginate, and functionalized with peripheral meniscus ECM.	<i>In vitro</i>	fibroblast differentiation was significantly increased in the outer zone and chondrogenic differentiation of stem cells was promoted in the inner zone.	[87]
	PCL/hydrogel/PDGF-BB/KGN	The 3D-printed PCL/hydrogel scaffold was dual-loaded with PDGF-BB and chondrogenic molecule KGN.	<i>In vitro</i> and <i>in vivo</i>	The heterogeneity was successfully achieved with the migration of ESPCs promoted by PDGF-BB and chondrogenic differentiation induced by KGN.	[88]
	PCL/MECM/KGN- $\mu\text{S}$	The 3D-printed PCL/MECM/KGN composite scaffold was loaded with PLGA $\mu\text{S}$ encapsulated with KGN.	<i>In vitro</i> and <i>in vivo</i>	The synergistic effect of MECM and KGN sustained release endows PCL/MECM-KGN $\mu\text{S}$ scaffold excellent cytocompatibility and chondrogenic activity.	[89]

(Contd...)

Table 2. (Continued)

Strategies combined with 3D printing	Materials	Methods and process	<i>In vitro</i> / <i>In vivo</i>	Biological effect of heterogeneity reconstruction	References
	PCL@ tetra-PEG	3D-printed polylactone/4 arm poly (ethylene glycol) hydrogel (PCL@ tetra-PEG) composite scaffold with Ac2-26 peptide coated.	<i>In vitro</i>	The anti-inflammatory and anti-oxidation effect in regulating the complex microenvironment and promote tissue regeneration were achieved.	[92]
	SF/PCL/L7	The MSC affinity peptide, LTHPRWP (L7), was combined with 3D-printed SF/PCL scaffold.	<i>In vitro</i> and <i>in vivo</i>	The scaffold promoted MSC proliferation, differentiation <i>in vitro</i> and biomimetic meniscus regeneration.	[96]
	SF/PVA/AESM	A multi-component composite SF/PVA scaffold was 3D-printed and combined with AESM.	<i>In vitro</i> and <i>in vivo</i>	AESM powder enhanced the biomechanical properties of the scaffold.	[97]
	PCL-DMECM	PCL scaffold and DMECM were combined with the assistance of 3D printing technique.	<i>In vitro</i> and <i>in vivo</i>	This dual-phase decellularized scaffold demonstrated great biocompatibility and biomechanical property, which further accelerate meniscus regeneration and delay osteoarthritis.	[108]
	PU/PCL/DMECM	Cell-loaded DMECM bioink and polyurethane (PU)-PCL were mixed for a 3D-printed TEM	<i>In vitro</i> and <i>in vivo</i>	The scaffold facilitated MSCs proliferation and fibrochondrogenic differentiation.	[109]
3D bioprinting	TCNF/ALG	The bioink consists of hMFC from the partial meniscectomy and TCNF/ALG.	<i>In vitro</i>	The expression of COL2A1 in TCNF/ALG construct was significantly increased.	[114]
	GG/FB/Sil-MA	The bioink consists of GG/FB and Sil-MA was 3D-bioprinted into a hybrid structure for fibrocartilage regeneration.	<i>In vitro</i> and <i>in vivo</i>	The regeneration of fibrocartilage tissue was promoted.	[115]
	GelMA/MECM	The meniscus derived bioink was combined with GelMA/MECM.	<i>In vitro</i> and <i>in vivo</i>	The scaffold showed sufficient feasibility and functionality in promoting cell viability, mechanical property, biodegradation and tissue formation.	[116]
	PCL/PLGA	3D-bioprinted anisotropic meniscus constructs with peripheral blood vessels growth and regional differential cell and ECM depositions were generated.	<i>In vitro</i> and <i>in vivo</i>	3D-bioprinted meniscus restored the anisotropy of native healthy meniscus with peripheral blood vessels infiltration.	[104]
Surface functional strategies	PLA/IPN	The surface of 3D-printed PLA scaffold was functionalized and embedded with self-healing IPN hydrogel for interface bonding.	<i>In vitro</i> and <i>in vivo</i>	The scaffold showed good biocompatibility and promoted meniscus tissue regeneration <i>in vivo</i> .	[117]
	PU/COL-1/FN	The surface of PU scaffolds was modified by physical absorption of COL-1 and FN.	<i>In vitro</i> and <i>in vivo</i>	FN coating was superior to COL-1 coating in promoting various stem cell functions, and FN was conducive to the formation of cartilage on scaffolds	[118]

(Contd...)

Table 2. (Continued)

Strategies combined with 3D printing	Materials	Methods and process	<i>In vitro</i> / <i>In vivo</i>	Biological effect of heterogeneity reconstruction	References
	PCL	The 3D-printed PCL scaffold was surface-etched by NaOH.	<i>In vitro</i>	Hydrophilic modification of scaffolds could improve the proliferation and adhesion of cells.	[119]
Bioreactors	PCL	The dynamic tension-compression system was designed to stimulate the biomimetic PCL scaffold biomechanically and biochemically.	<i>In vitro</i> and <i>in vivo</i>	Anisotropic cell phenotype in PCL scaffold was successfully achieved, and articular cartilage was inspiringly protected	[127]
Growth factors	PCL	3D-printed PCL scaffold was loaded with CTGF in the outer and TGF- $\beta$ 3 in the inner region.	<i>In vitro</i> and <i>in vivo</i>	BMSCs differentiated towards chondrocytes and fibrochondrocytes heterogeneously.	[93]
	PCL	3D-printed PCL scaffold was loaded with CTGF in the outer and TGF- $\beta$ 4 in the inner region.	<i>In vivo</i>	After 1 year implantation in sheep knee, f12MRI showed scaffold extrusion.	[132]

TEM: Tissue-engineered menisci, PCL: Poly( $\epsilon$ -caprolactone)

systems can quantify stresses and strains on specific structures or tissues<sup>[119-121]</sup>. A model closer to heterogeneity better explains the biological action patterns. Therefore, bioreactors simulating specific microenvironments are widely used in bioengineering<sup>[122]</sup>, among which bioreactors mimicking knee joints have already been studied for meniscus regeneration and biomechanical changes post-meniscectomy<sup>[123,124]</sup>. Region-dependent mechanical and chemical stimulations are effective ways to construct heterogeneous TEM for meniscal regeneration<sup>[125]</sup>.

A dynamic tension-compression system was designed for heterogeneous TEM reconstruction. Together with the two growth factors, the MSCs in the biomimetic PCL scaffold were biomechanically and biochemically stimulated with the aim of inducing a spatially heterogeneous distribution of chondrocytes. The results showed that the anisotropic cell phenotype in the PCL scaffold was successfully achieved, and the knee joint cartilage was protected<sup>[126]</sup>.

Nonetheless, there is still a long way for TEM from laboratory to clinic, with obstacles to be removed, such as concise statistics and parameters for bioreactors and sophisticated interactions between biomechanical contact and cell bioaction<sup>[119]</sup>. Furthermore, more impactful research is necessary to gain insight into the criteria and parameters of bioreactors.

### 3.6. Growth factors applied for 3D-printed heterogeneous TEM

Growth factors, recognized as indispensable regulators of cell and tissue growth, play a critical role in specific

tissue formation by inducing the specific differentiation of endogenous stem/progenitor cells. Accordingly, growth factors have been utilized in bioengineering to promote tissue regeneration. For instance, diverse growth factors have been regionally added to the TEM. Studies have highlighted the importance of CTGF that plays an indispensable role in the fibrochondrogenic differentiation of stem cells, while TGF $\beta$ 3 promotes hyaline chondrogenic differentiation<sup>[127-130]</sup>.

Lee *et al.* fabricated a 3D-printed PCL scaffold loaded with CTGF in the outer region and TGF- $\beta$ 3 in the inner region. By controlling the release of specific growth factors, bone marrow-derived MSCs (BMSCs) successfully differentiate into chondrocytes and fibrochondrocytes heterogeneously. They further detected the bioeffect *in vivo* by implanting this heterogeneous TEM into ovine knee joints, showing that significantly increased COL-1 and COL2 levels were successfully induced by CTGF and TGF $\beta$ 3, respectively<sup>[131]</sup>. Nakagawa *et al.* also evaluated the long-term *in vivo* effect of loading 3D printing PCL meniscus scaffold loaded with CTGF and TGF- $\beta$ 3 in an ovine knee meniscectomy model for up to 1 year. However, MRI showed that most scaffolds were extruded, which may lead to cartilage degeneration in the treatment group<sup>[132]</sup>. In addition, growth factors, although accelerating the development of bioengineering, are still at risk of disease transmission because of their exogenous characteristics. Excavation of autologous biomaterials with growth factor-like functions and low immunogenicity is required. The 3D printing strategies of heterogeneous TEM are summarized in Table 2.

## 4. Conclusion

Meniscus tears are one of the most common injuries in sports medicine and can lead to pain, swelling, locking, and movement disorders of the knee joint. For meniscus tear, although a few cases can be sutured, partial or total meniscectomy is still the main treatment method, which will significantly increase the risk of osteoarthritis. Allogeneic meniscus transplantation can improve joint function and relieve symptoms such as pain and swelling after meniscectomy, but there are still many limitations, such as insufficient donor source, potential immune rejection, and uncertain long-term follow-up efficacy. Meniscus prostheses, such as CMI<sup>®</sup>, Actifit<sup>®</sup>, and NUSurface<sup>®</sup>, although applied clinically, do not work well in long-term implantation. TEM has become an emerging strategy to overcome this challenge and 3D printing is a promising strategy due to its efficacy, cost-effectiveness, controllability, and diversity of selectable materials. Novel manufacturing techniques that combine multiple biomaterials and apply bioreactors, 3D bioprinting, surface functionalization, and growth factors are effective ways to realize the heterogeneity of TEM.

However, there are still some challenges and limitations in terms of the meniscus tissue engineering strategies. As discussed before, the meniscus is a fibrocartilaginous tissue within the knee joint and performs several critical biofunctions, preventing the knee joint cartilage degeneration. These crucial biofunctions were largely generated by the special heterogeneity of natural meniscus, including biological and biomechanical heterogeneities. Therefore, the functional meniscus reconstruction is essential for the successful cartilage protection and alleviation of knee joint osteoarthritis. However, the current tissue engineering approaches of meniscus reconstruction still cannot concurrently realize the biological and biomechanical reconstruction, so the meniscus biofunctions in the knee joint cannot be restored and the osteoarthritis induced by meniscus injury cannot be alleviated consequently. Thus, in future research concerning TEM, scientists should take the biofunction restoration of natural meniscus into consideration, instead of reconstructing the meniscus with biological and biomechanical heterogeneities separately. In addition, considering the clinical promotion of the TEM products, the practicability, simplicity, safety, and functionality of that still need to be further explored.

## Funding

The authors would like to acknowledge financial support from the National Key Research and Development Program of China (Grant No. 2019YFB1706900), National Natural Science Foundation of China (82102565, 82072428), and Natural Science Foundation of Beijing Municipality (7212132).

## Conflict of interest

The authors declare that the research was conducted in the absence of any commercial or financial relationships that could be construed as potential conflicts of interest.

## Author contributions

*Conceptualization:* Dong Jiang, You-Rong Chen  
*Formal analysis:* Li-Ya Ai, Tong Su, Zhen Zhang. *Writing – original draft:* Ming-Ze Du, Yun Dou  
*Writing – review and editing:* You-Rong Chen, Dong Jiang

All authors approved the final version for publication.

## Ethics approval and consent to participate

Not applicable.

## Consent for publication

Not applicable.

## Availability of data

All data that support the findings of this work are included within the article.

## References

1. Syed S, Zaki MN, Lakshmanan J, *et al.*, 2022, Knee meniscal retears after repair: A systematic review comparing diagnostic imaging modalities. *Libyan J Med*, 17: 2030024.  
<https://doi.org/10.1080/19932820.2022.2030024>
2. Gee SM, Posner M, 2021, Meniscus anatomy and basic science. *Sports Med Arthrosc Rev*, 29: e18–23.  
<https://doi.org/10.1097/jsa.0000000000000327>
3. Canciani B, Millar VR, Pallaoro M, *et al.*, 2021, Testing hypoxia in pig meniscal culture: Biological role of the vascular-related factors in the differentiation and viability of neonatal meniscus. *Int J Mol Sci*, 22: 12465.  
<https://doi.org/10.3390/ijms222212465>
4. Logerstedt DS, Ebert JR, MacLeod TD, *et al.*, 2022, Effects of and response to mechanical loading on the knee. *Sports Med*, 52: 201–235.  
<https://doi.org/10.1007/s40279-021-01579-7>
5. Morejon A, Mantero AM, Best TM, *et al.*, 2022, Mechanisms of energy dissipation and relationship with tissue composition in human meniscus. *Osteoarthritis Cartilage*, 30: 605–612.  
<https://doi.org/10.1016/j.joca.2022.01.001>
6. Hart DA, Nakamura N, Shrive NG, 2021, Perspective: Challenges presented for regeneration of heterogeneous musculoskeletal tissues that normally develop in unique biomechanical environments. *Front Bioeng Biotechnol*,

- 9: 760273.  
<https://doi.org/10.3389/fbioe.2021.760273>
7. Perrone D, 1946, Upon a case of right internal meniscus injur; meniscectomy. *Med Cir Farm*, 8: 20–23.
  8. Garrett WE Jr, Swiontkowski MF, Weinstein JN, *et al.*, 2006, American Board of Orthopaedic Surgery Practice of the Orthopaedic Surgeon: Part-II, certification examination case mix. *J Bone Joint Surg Am*, 88: 660–667.  
<https://doi.org/10.2106/00004623-200603000-00027>
  9. Sheffield R, 1978, Community health education fostered by hospital program. *Hospitals*, 52: 113–114, 118–119.
  10. Brutico JM, Wright ML, Kamel SI, *et al.*, 2021, The relationship between discoid meniscus and articular cartilage thickness: A quantitative observational study with MRI. *Orthop J Sports Med*, 9: 23259671211062256.  
<https://doi.org/10.1177/23259671211062258>
  11. Poulsen E, Goncalves GH, Bricca A, *et al.*, 2019, Knee osteoarthritis risk is increased 4–6 fold after knee injury—a systematic review and meta-analysis. *Br J Sports Med*, 53: 1454–1463.  
<https://doi.org/10.1136/bjsports-2018-100022>
  12. Pattappa G, Johnstone B, Zellner J, *et al.*, 2019, The importance of physioxia in mesenchymal stem cell chondrogenesis and the mechanisms controlling its response. *Int J Mol Sci*, 20: E484.  
<https://doi.org/10.3390/ijms20030484>
  13. Travascio F, Jackson AR, 2017, The nutrition of the human meniscus: A computational analysis investigating the effect of vascular recession on tissue homeostasis. *J Biomech*, 61: 151–159.  
<https://doi.org/10.1016/j.jbiomech.2017.07.019>
  14. Di Giancamillo A, Deponti D, Modina S, *et al.*, 2017, Age-related modulation of angiogenesis-regulating factors in the swine meniscus. *J Cell Mol Med*, 21: 3066–3075.  
<https://doi.org/10.1111/jcmm.13218>
  15. Monllau JC, Poggioli F, Erquicia J, *et al.*, 2018, Magnetic resonance imaging and functional outcomes after a polyurethane meniscal scaffold implantation: Minimum 5-year follow-up. *Arthroscopy*, 34: 1621–1627.  
<https://doi.org/10.1016/j.arthro.2017.12.019>
  16. Houck DA, Kraeutler MJ, Belk JW, *et al.*, 2018, Similar clinical outcomes following collagen or polyurethane meniscal scaffold implantation: A systematic review. *Knee Surg Sports Traumatol Arthrosc*, 26: 2259–2269.  
<https://doi.org/10.1007/s00167-018-4838-1>
  17. Perera K, Ivone R, Natekin E, *et al.*, 2021, 3D bioprinted implants for cartilage repair in intervertebral discs and knee menisci. *Front Bioeng Biotechnol*, 9: 754113.  
<https://doi.org/10.3389/fbioe.2021.754113>
  18. Dai W, Wu T, Leng X, *et al.*, 2021, Advances in biomechanical and biochemical engineering methods to stimulate meniscus tissue. *Am J Transl Res*, 13: 8540–8560.
  19. Kwon H, Brown WE, Lee CA, *et al.*, 2019, Surgical and tissue engineering strategies for articular cartilage and meniscus repair. *Nat Rev Rheumatol*, 15: 550–570.  
<https://doi.org/10.1038/s41584-019-0255-1>
  20. Smith BD, Grande DA, 2015, The current state of scaffolds for musculoskeletal regenerative applications. *Nat Rev Rheumatol*, 11: 213–222.  
<https://doi.org/10.1038/nrrheum.2015.27>
  21. Makris EA, Hadidi P, Athanasiou KA, 2011, The knee meniscus: Structure-function, pathophysiology, current repair techniques, and prospects for regeneration. *Biomaterials*, 32: 7411–7431.  
<https://doi.org/10.1016/j.biomaterials.2011.06.037>
  22. Wang H, Wang Z, Liu H, *et al.*, 2021, Three-dimensional printing strategies for irregularly shaped cartilage tissue engineering: Current state and challenges. *Front Bioeng Biotechnol*, 9: 777039.  
<https://doi.org/10.3389/fbioe.2021.777039>
  23. Bryceland JK, Powell AJ, Nunn T, 2017, Knee menisci. *Cartilage*, 8: 99–104.  
<https://doi.org/10.1177/1947603516654945>
  24. Fox AJ, Bedi A, Rodeo SA, 2012, The basic science of human knee menisci: Structure, composition, and function. *Sports Health*, 4: 340–351.  
<https://doi.org/10.1177/1941738111429419>
  25. Li Q, Qu F, Han B, *et al.*, 2017, Micromechanical anisotropy and heterogeneity of the meniscus extracellular matrix. *Acta Biomater*, 54: 356–366.  
<https://doi.org/10.1016/j.actbio.2017.02.043>
  26. Han WM, Heo SJ, *et al.*, 2016, Microstructural heterogeneity directs micromechanics and mechanobiology in native and engineered fibrocartilage. *Nat Mater*, 15: 477–484.  
<https://doi.org/10.1038/nmat4520>
  27. Leslie BW, Gardner DL, McGeough JA, *et al.*, 2000, Anisotropic response of the human knee joint meniscus to unconfined compression. *Proc Inst Mech Eng H*, 214: 631–635.  
<https://doi.org/10.1243/0954411001535651>
  28. Coluccino L, Peres C, Gottardi R, *et al.*, 2017, Anisotropy in the viscoelastic response of knee meniscus cartilage. *J Appl Biomater Funct Mater*, 15: e77–e83.  
<https://doi.org/10.5301/jabfm.5000319>
  29. Gardner E, O’Rahilly R, 1968, The early development of the

- knee joint in staged human embryos. *J Anat*, 102: 289–299.
30. McDermott ID, Sharifi F, Bull AM, *et al.*, 2004, An anatomical study of meniscal allograft sizing. *Knee Surg Sports Traumatol Arthrosc*, 12: 130–135.  
<https://doi.org/10.1007/s00167-003-0366-7>
31. Shaffer B, Kennedy S, Klimkiewicz J, *et al.*, 2000, Preoperative sizing of meniscal allografts in meniscus transplantation. *Am J Sports Med*, 28: 524–533.  
<https://doi.org/10.1177/03635465000280041301>
32. Clark CR, Ogden JA, 1983, Development of the menisci of the human knee joint. Morphological changes and their potential role in childhood meniscal injury. *J Bone Joint Surg Am*, 65: 538–547.  
<https://doi.org/10.2106/0004623-198365040-00018>
33. Natsis K, Karasavvidis T, Kola D, *et al.*, 2020, Menisofibular ligament: How much do we know about this structure of the posterolateral corner of the knee: Anatomical study and review of literature. *Surg Radiol Anat*, 42: 1203–1208.  
<https://doi.org/10.1007/s00276-020-02459-x>
34. Guy S, Ferreira A, Carrozzo A, *et al.*, 2022, Isolated meniscotibial ligament rupture: The medial meniscus “Belt Lesion.” *Arthrosc Tech*, 11: e133–e138.  
<https://doi.org/10.1016/j.eats.2021.09.013>
35. Arner JW, Ruzbarsky JJ, Vidal AF, *et al.*, 2022, Meniscus repair part 1: Biology, function, tear morphology, and special considerations. *J Am Acad Orthop Surg*, 30: e852–e858.  
<https://doi.org/10.5435/jaas-d-21-00993>
36. Gee SM, Posner M, 2021, Meniscus anatomy and basic science. *Sports Med Arthrosc Rev*, 29: e18–e23.  
<https://doi.org/10.1097/jsa.0000000000000327>
37. Abbadessa A, Crecente-Campo J, Alonso MJ, 2021, Engineering anisotropic meniscus: Zonal functionality and spatiotemporal drug delivery. *Tissue Eng Part B Rev*, 27: 133–154.  
<https://doi.org/10.1089/ten.teb.2020.0096>
38. Williams LB, Adesida AB, 2018, Angiogenic approaches to meniscal healing. *Injury*, 49: 467–472.  
<https://doi.org/10.1016/j.injury.2018.01.028>
39. Roughley PJ, 2006, The structure and function of cartilage proteoglycans. *Eur Cell Mater*, 12: 92–101.
40. Dye SF, Vaupel GL, Dye CC, 1998, Conscious neurosensory mapping of the internal structures of the human knee without intraarticular anesthesia. *Am J Sports Med*, 26: 773–777.  
<https://doi.org/10.1177/03635465980260060601>
41. Herwig J, Egner E, Buddecke E, 1984, Chemical changes of human knee joint menisci in various stages of degeneration. *Ann Rheum Dis*, 43: 635–640.  
<https://doi.org/10.1136/ard.43.4.635>
42. Proctor CS, Schmidt MB, Whipple RR, *et al.*, 1989, Material properties of the normal medial bovine meniscus. *J Orthop Res*, 7: 771–782.  
<https://doi.org/10.1002/jor.1100070602>
43. Sweigart MA, Athanasiou KA, 2001, Toward tissue engineering of the knee meniscus. *Tissue Eng*, 7: 111–129.  
<https://doi.org/10.1089/107632701300062697>
44. McDevitt CA, Webber RJ, 1990, The ultrastructure and biochemistry of meniscal cartilage. *Clin Orthop Relat Res*, 252: 8–18.
45. Miller GK, 1996, A prospective study comparing the accuracy of the clinical diagnosis of meniscus tear with magnetic resonance imaging and its effect on clinical outcome. *Arthroscopy*, 12: 406–413.  
[https://doi.org/10.1016/s0749-8063\(96\)90033-x](https://doi.org/10.1016/s0749-8063(96)90033-x)
46. Li H, Wang X, Liu J, *et al.*, 2021, Nanofiber configuration affects biological performance of decellularized meniscus extracellular matrix incorporated electrospun scaffolds. *Biomed Mater*, 16: 065013.  
<https://doi.org/10.1088/1748-605x/ac28a5>
47. Ghadially FN, Lalonde JM, Wedge JH, 1983, Ultrastructure of normal and torn menisci of the human knee joint. *J Anat*, 136: 773–791.
48. Ghadially FN, Thomas I, Yong N, 1978, Ultrastructure of rabbit semilunar cartilages. *J Anat*, 125: 499–517.
49. Le Graverand MP, Ou Y, Schield-Yee T, *et al.*, 2001, The cells of the rabbit meniscus: Their arrangement, interrelationship, morphological variations and cytoarchitecture. *J Anatomy*, 198: 525–535.  
<https://doi.org/10.1046/j.1469-7580.2000.19850525.x>
50. Zhang X, Aoyama T, Ito A, *et al.*, 2014, Regional comparisons of porcine menisci. *J Orthop Res*, 32: 1602–1611.  
<https://doi.org/10.1002/jor.22687>
51. Vanderploeg EJ, Wilson CG, Imler SM, *et al.*, 2012, Regional variations in the distribution and colocalization of extracellular matrix proteins in the juvenile bovine meniscus. *J Anat*, 221: 174–186.  
<https://doi.org/10.1111/j.1469-7580.2012.01523.x>
52. Di Giancamillo A, Deponti D, Addis A, *et al.*, 2014, Meniscus maturation in the swine model: Changes occurring along with anterior to posterior and medial to lateral aspect during growth. *J Cell Mol Med*, 18: 1964–1974.  
<https://doi.org/10.1111/jcmm.12367>
53. Zhang Z, Guo W, Gao S, *et al.*, 2018, Native tissue-based strategies for meniscus repair and regeneration. *Cell Tissue Res*, 373: 337–350.  
<https://doi.org/10.1007/s00441-017-2778-6>



54. Pillai MM, Gopinathan J, Selvakumar R, *et al.*, 2018, Human knee meniscus regeneration strategies: A review on recent advances. *Curr Osteoporos Rep*, 16: 224–235.  
<https://doi.org/10.1007/s11914-018-0436-x>
55. Seitz AM, Galbusera F, Kraus C, *et al.*, 2013, Stress-relaxation response of human menisci under confined compression conditions. *J Mech Behav Biomed Mater*, 26: 68–80.  
<https://doi.org/10.1016/j.jmbbm.2013.09.012>
56. Higashioka MM, Chen JA, Hu JC, *et al.*, 2014, Building an anisotropic meniscus with zonal variations. *Tissue Eng Part A*, 20: 294–302.  
<https://doi.org/10.1089/ten.tea.2013.0098>
57. Ahmed AM, Burke DL, 1983, *In-vitro* measurement of static pressure distribution in synovial joints--part I: Tibial surface of the knee. *J Biomech Eng*, 105: 216–225.  
<https://doi.org/10.1115/1.3138409>
58. Shrive NG, O'Connor JJ, Goodfellow JW, 1978, Load-bearing in the knee joint. *Clin Orthop Relat Res*, 131: 279–287.
59. Kurosawa H, Fukubayashi T, Nakajima H, 1980, Load-bearing mode of the knee joint: Physical behavior of the knee joint with or without menisci. *Clin Orthop Relat Res*, 149, 283–290.  
<https://doi.org/10.1097/00003086-198006000-00039>
60. Kawahara Y, Uetani M, Fuchi K, *et al.*, 1999, MR assessment of movement and morphologic change in the menisci during knee flexion. *Acta Radiol*, 40: 610–614.  
<https://doi.org/10.3109/02841859909175596>
61. Freutel M, Seitz AM, Galbusera F, *et al.*, 2014, Medial meniscal displacement and strain in three dimensions under compressive loads: MR assessment: 3D Displacement and strain of the meniscus. *J Magn Reson Imaging*, 40: 1181–1188.  
<https://doi.org/10.1002/jmri.24461>
62. Beaupré A, Choukroun R, Guidouin R, *et al.*, 1986, Knee menisci. Correlation between microstructure and biomechanics. *Clin Orthop Relat Res*, 208: 72–75.  
<https://doi.org/10.1097/00003086-198607000-00016>
63. Bullough PG, Munuera L, Murphy J, *et al.*, 1970, The strength of the menisci of the knee as it relates to their fine structure. *J Bone Joint Surg Br*, 52: 564–567.  
<https://doi.org/10.1302/0301-620x.52b3.564>
64. Moyer JT, Priest R, Bouman T, *et al.*, 2013, Indentation properties and glycosaminoglycan content of human menisci in the deep zone. *Acta Biomater*, 9: 6624–6629.  
<https://doi.org/10.1016/j.actbio.2012.12.033>
65. Gonzalez-Leon EA, Hu JC, Athanasiou KA, 2022, Yucatan minipig knee meniscus regional biomechanics and biochemical structure support its suitability as a large animal model for translational research. *Front Bioeng Biotechnol*, 10: 844416.  
<https://doi.org/10.3389/fbioe.2022.844416>
66. Skaggs DL, Warden WH, Mow VC, 1994, Radial Tie fibers influence the tensile properties of the bovine medial meniscus. *J Orthop Res*, 12: 176–185.  
<https://doi.org/10.1002/jor.1100120205>
67. Joshi MD, Suh JK, Marui T, *et al.*, 1995, Interspecies variation of compressive biomechanical properties of the meniscus. *J Biomed Mater Res*, 29: 823–828.  
<https://doi.org/10.1002/jbm.820290706>
68. Danso EK, Mäkelä JT, Tanska P, *et al.*, 2015, Characterization of site-specific biomechanical properties of human meniscus-importance of collagen and fluid on mechanical nonlinearities. *J Biomech*, 48: 1499–1507.  
<https://doi.org/10.1016/j.jbiomech.2015.01.048>
69. Berni M, Marchiori G, Cassiolas G, *et al.*, 2021, Anisotropy and inhomogeneity of permeability and fibrous network response in the pars intermedia of the human lateral meniscus. *Acta Biomater*, 135: 393–402.  
<https://doi.org/10.1016/j.actbio.2021.08.020>
70. Upton ML, Hennerbichler A, Fermor B, *et al.*, 2006, Biaxial strain effects on cells from the inner and outer regions of the meniscus. *Connect Tissue Res*, 47: 207–214.  
<https://doi.org/10.1080/03008200600846663>
71. Furumatsu T, Kanazawa T, Miyake Y, *et al.*, 2012, Mechanical stretch increases Smad3-dependent CCN2 expression in inner meniscus cells: Stretch-induced CCN2 in the meniscus. *J Orthop Res*, 30: 1738–1745.  
<https://doi.org/10.1002/jor.22142>
72. Guo W, Liu S, Zhu Y, *et al.*, 2015, Advances and prospects in tissue-engineered meniscal scaffolds for meniscus regeneration. *Stem Cells Int*, 2015: 517520.  
<https://doi.org/10.1155/2015/517520>
73. Vasiliadis AV, Koukoulis N, Katakalos K, 2021, Three-dimensional-printed scaffolds for meniscus tissue engineering: Opportunity for the future in the orthopaedic world. *J Funct Biomater*, 12: 69.  
<https://doi.org/10.3390/jfb12040069>
74. Yang Y, Chen Z, Song X, *et al.*, 2017, Biomimetic anisotropic reinforcement architectures by electrically assisted nanocomposite 3D printing. *Adv Mater*, 29: 1605750.  
<https://doi.org/10.1002/adma.201770076>
75. Bahcecioglu G, Bilgen B, Hasirci N, *et al.*, 2019, Anatomical meniscus construct with zone specific biochemical composition and structural organization. *Biomaterials*, 218: 119361.  
<https://doi.org/10.1016/j.biomaterials.2019.119361>

76. Din US, Sian TS, Deane CS, *et al.*, 2021, Green tea extract concurrent with an oral nutritional supplement acutely enhances muscle microvascular blood flow without altering leg glucose uptake in healthy older adults. *Nutrients*, 13: 3895.  
<https://doi.org/10.3390/nu13113895>
77. Terpstra ML, Li J, Mensinga A, *et al.*, 2022, Bioink with cartilage-derived extracellular matrix microfibers enables spatial control of vascular capillary formation in bioprinted constructs. *Biofabrication*, 14: 034104.  
<https://doi.org/10.1088/1758-5090/ac6282>
78. Kumar G, Tison CK, Chatterjee K, *et al.*, 2011, The determination of stem cell fate by 3D scaffold structures through the control of cell shape. *Biomaterials*, 32: 9188–9196.  
<https://doi.org/10.1016/j.biomaterials.2011.08.054>
79. Neffe AT, Pierce BF, Tronci G, *et al.*, 2015, One step creation of multifunctional 3D architected hydrogels inducing bone regeneration. *Adv Mater*, 27: 1738–1744.  
<https://doi.org/10.1002/adma.201404787>
80. Zhang ZZ, Jiang D, Ding JX, *et al.*, 2016, Role of scaffold mean pore size in meniscus regeneration. *Acta Biomater*, 43: 314–326.  
<https://doi.org/10.1016/j.actbio.2016.07.050>
81. Di Luca A, Szlazak K, Lorenzo-Moldero I, *et al.*, 2016, Influencing chondrogenic differentiation of human mesenchymal stromal cells in scaffolds displaying a structural gradient in pore size. *Acta Biomater*, 36: 210–219.  
<https://doi.org/10.1016/j.actbio.2016.03.014>
82. van der Wal WA, Meijer DT, Hoogeslag RA, *et al.*, 2022, Meniscal tears, posterolateral and posteromedial corner injuries, increased coronal plane, and increased sagittal plane tibial slope all influence anterior cruciate ligament-related knee kinematics and increase forces on the native and reconstructed anterior cruciate ligament: A Systematic review of cadaveric studies. *Arthroscopy*, 38: 1664–1688.e1.  
<https://doi.org/10.1016/j.arthro.2021.11.044>
83. Stocco TD, Silva MC, Corat MA, *et al.*, 2022, Towards bioinspired meniscus-regenerative scaffolds: Engineering a novel 3D bioprinted patient-specific construct reinforced by biomimetically aligned nanofibers. *Int J Nanomed*, 17: 1111–1124.  
<https://doi.org/10.2147/ijn.s353937>
84. Cengiz IF, Maia FR, da Silva Morais A, *et al.*, 2020, Entrapped in cage (EiC) scaffolds of 3D-printed polycaprolactone and porous silk fibroin for meniscus tissue engineering. *Biofabrication*, 12: 025028.  
<https://doi.org/10.1088/1758-5090/ab779f>
85. Li H, Li P, Yang Z, *et al.*, 2021, Meniscal regenerative scaffolds based on biopolymers and polymers: Recent status and applications. *Front Cell Dev Biol*, 9: 661802.  
<https://doi.org/10.3389/fcell.2021.661802>
86. Bahcecioglu G, Hasirci N, Bilgen B, *et al.*, 2019, A 3D printed PCL/hydrogel construct with zone-specific biochemical composition mimicking that of the meniscus. *Biofabrication*, 11: 025002.  
<https://doi.org/10.1088/1758-5090/aaf707>
87. Romanazzo S, Vedicherla S, Moran C, *et al.*, 2018, Meniscus ECM-functionalised hydrogels containing infrapatellar fat pad-derived stem cells for bioprinting of regionally defined meniscal tissue. *J Tissue Eng Regen Med*, 12: e1826–e1835.  
<https://doi.org/10.1002/term.2602>
88. Li H, Liao Z, Yang Z, *et al.*, 2021, 3D printed poly( $\epsilon$ -caprolactone)/meniscus extracellular matrix composite scaffold functionalized with kartogenin-releasing PLGA microspheres for meniscus tissue engineering. *Front Bioeng Biotechnol*, 9: 662381.  
<https://doi.org/10.3389/fbioe.2021.662381>
89. Hao L, Tianyuan Z, Zhen Y, *et al.*, 2021, Biofabrication of cell-free dual drug-releasing biomimetic scaffolds for meniscal regeneration. *Biofabrication*, 14: 015001.  
<https://doi.org/10.1088/1758-5090/ac2cd7>
90. Gomes JM, Silva SS, Fernandes EM, *et al.*, 2022, Silk fibroin/cholinium gallate-based architectures as therapeutic tools. *Acta Biomater*, 147: 168–184.  
<https://doi.org/10.1016/j.actbio.2022.05.020>
91. Yu Q, Han F, Yuan Z, *et al.*, 2022, Fucoidan-loaded nanofibrous scaffolds promote annulus fibrosus repair by ameliorating the inflammatory and oxidative microenvironments in degenerative intervertebral discs. *Acta Biomater*, 148: 73–89.  
<https://doi.org/10.1016/j.actbio.2022.05.054>
92. Xu B, Ye J, Fan BS, *et al.*, 2023, Protein-spatiotemporal partition releasing gradient porous scaffolds and anti-inflammatory and antioxidant regulation remodel tissue engineered anisotropic meniscus. *Bioact Mater*, 20: 194–207.  
<https://doi.org/10.1016/j.bioactmat.2022.05.019>
93. Lammel AS, Hu X, Park SH, *et al.*, 2010, Controlling silk fibroin particle features for drug delivery. *Biomaterials*, 31: 4583–4591.  
<https://doi.org/10.1016/j.biomaterials.2010.02.024>
94. Gou S, Chen N, Wu X, *et al.*, 2022, Multi-responsive nanotheranostics with enhanced tumor penetration and oxygen self-producing capacities for multimodal synergistic cancer therapy. *Acta Pharm Sin B*, 12: 406–423.  
<https://doi.org/10.1016/j.apsb.2021.07.001>
95. Li Z, Wu N, Cheng J, *et al.*, 2020, Biomechanically, structurally and functionally meticulously tailored polycaprolactone/silk fibroin scaffold for meniscus regeneration. *Theranostics*,

- 10: 5090–5106.  
<https://doi.org/10.7150/thno.44270>
96. Pillai MM, Gopinathan J, Kumar RS, *et al.*, 2018, Tissue engineering of human knee meniscus using functionalized and reinforced silk-polyvinyl alcohol composite three-dimensional scaffolds: Understanding the *in vitro* and *in vivo* behavior. *J Biomed Mater Res A*, 106: 1722–1731.  
<https://doi.org/10.1002/jbm.a.36372>
97. Spang MT, Christman KL, 2018, Extracellular matrix hydrogel therapies: *In vivo* applications and development. *Acta Biomater*, 68: 1–14.  
<https://doi.org/10.1016/j.actbio.2017.12.019>
98. Hu X, Xia Z, Cai K, 2022, Recent advances in 3D hydrogel culture systems for mesenchymal stem cell-based therapy and cell behavior regulation. *J Mater Chem B*, 10: 1486–1507.  
<https://doi.org/10.1039/D1TB02537F>
99. Yu Z, Lili J, Tiezheng Z, *et al.*, 2019, Development of decellularized meniscus extracellular matrix and gelatin/chitosan scaffolds for meniscus tissue engineering. *Biomed Mater Eng*, 30: 125–132.  
<https://doi.org/10.3233/bme-191038>
100. Gao S, Guo W, Chen M, *et al.*, 2017, Fabrication and characterization of electrospun nanofibers composed of decellularized meniscus extracellular matrix and polycaprolactone for meniscus tissue engineering. *J Mater Chem B*, 5: 2273–2285.  
<https://doi.org/10.1039/c6tb03299k>
101. Shimomura K, Rothrauff BB, Tuan RS, 2017, Region-specific effect of the decellularized meniscus extracellular matrix on mesenchymal stem cell-based meniscus tissue engineering. *Am J Sports Med*, 45: 604–611.  
<https://doi.org/10.1177/0363546516674184>
102. Gao S, Yuan Z, Guo W, *et al.*, 2017, Comparison of glutaraldehyde and carbodiimides to crosslink tissue engineering scaffolds fabricated by decellularized porcine menisci. *Mater Sci Eng C Mater Biol Appl*, 71: 891–900.  
<https://doi.org/10.1016/j.msec.2016.10.074>
103. Sun Y, Zhang Y, Wu Q, *et al.*, 2021, 3D-bioprinting ready-to-implant anisotropic menisci recapitulate healthy meniscus phenotype and prevent secondary joint degeneration. *Theranostics*, 11: 5160–5173.  
<https://doi.org/10.7150/thno.54864>
104. Xia B, Kim DH, Bansal S, *et al.*, 2021, Development of a decellularized meniscus matrix-based nanofibrous scaffold for meniscus tissue engineering. *Acta Biomater*, 128: 175–185.  
<https://doi.org/10.1016/j.actbio.2021.03.074>
105. Wu J, Xu J, Huang Y, *et al.*, 2021, Regional-specific meniscal extracellular matrix hydrogels and their effects on cell-matrix interactions of fibrochondrocytes. *Biomed Mater*, 17: 014105.  
<https://doi.org/10.1088/1748-605x/ac4178>
106. Zhong G, Yao J, Huang X, *et al.*, 2020, Injectable ECM hydrogel for delivery of BMSCs enabled full-thickness meniscus repair in an orthotopic rat model. *Bioact Mater*, 5: 871–879.  
<https://doi.org/10.1016/j.bioactmat.2020.06.008>
107. Guo W, Chen M, Wang Z, *et al.*, 2021, 3D-printed cell-free PCL-MECM scaffold with biomimetic micro-structure and micro-environment to enhance *in situ* meniscus regeneration. *Bioact Mater*, 6: 3620–3633.  
<https://doi.org/10.1016/j.bioactmat.2021.02.019>
108. Vassiliou G, 1986, Current concepts of cervical fractures of the teeth and their treatment. *Stomatologia (Athenai)*, 43: 399–411.
109. Rothrauff BB, Shimomura K, Gottardi R, *et al.*, 2017, Anatomical region-dependent enhancement of 3-dimensional chondrogenic differentiation of human mesenchymal stem cells by soluble meniscus extracellular matrix. *Acta Biomater*, 49: 140–151.  
<https://doi.org/10.1016/j.actbio.2016.11.046>
110. Zhang CY, Fu CP, Li XY, *et al.*, 2022, Three-dimensional bioprinting of decellularized extracellular matrix-based bioinks for tissue engineering. *Molecules*, 27: 3442.  
<https://doi.org/10.3390/molecules27113442>
111. Szojka A, Lalh K, Andrews SH, *et al.*, 2017, Biomimetic 3D printed scaffolds for meniscus tissue engineering. *Bioprinting*, 8: 1–7.  
<https://doi.org/10.1016/j.bprint.2017.08.001>
112. Sooriyaarachchi D, Wu J, Feng A, *et al.*, 2019, Hybrid fabrication of biomimetic meniscus scaffold by 3D printing and parallel electrospinning. *Proc Manuf*, 34: 528–534.  
<https://doi.org/10.1016/j.promfg.2019.06.216>
113. Lan X, Ma Z, Szojka AR, *et al.*, 2021, TEMPO-oxidized cellulose nanofiber-alginate hydrogel as a bioink for human meniscus tissue engineering. *Front Bioeng Biotechnol*, 9: 766399.  
<https://doi.org/10.3389/fbioe.2021.766399>
114. Costa JB, Park J, Jorgensen AM, *et al.*, 2020, 3D bioprinted highly elastic hybrid constructs for advanced fibrocartilaginous tissue regeneration. *Chem Mater*, 32: 8733–8746.  
<https://doi.org/10.1021/acs.chemmater.0c03556>
115. Jian Z, Zhuang T, Qinyu T, *et al.*, 2021, 3D bioprinting of a biomimetic meniscal scaffold for application in tissue engineering. *Bioact Mater*, 6: 1711–1726.

- <https://doi.org/10.1016/j.bioactmat.2020.11.027>
116. Gupta S, Sharma A, Kumar JV, *et al.*, 2020, Meniscal tissue engineering via 3D printed PLA monolith with carbohydrate based self-healing interpenetrating network hydrogel. *Int J Biol Macromol*, 162: 1358–13571.  
<https://doi.org/10.1016/j.ijbiomac.2020.07.238>
117. Deng X, Chen X, Geng F, *et al.*, 2021, Precision 3D printed meniscus scaffolds to facilitate hMSCs proliferation and chondrogenic differentiation for tissue regeneration. *J Nanobiotechnology*, 19: 400.  
<https://doi.org/10.1186/s12951-021-01141-7>
118. Zhou ZX, Chen YR, Zhang JY, *et al.*, 2020, Facile strategy on hydrophilic modification of poly( $\epsilon$ -caprolactone) scaffolds for assisting tissue-engineered meniscus constructs *in vitro*. *Front Pharmacol*, 11: 471.  
<https://doi.org/10.3389/fphar.2020.00471>
119. Rodeo SA, Monibi F, Dehghani B, *et al.*, 2020, Biological and mechanical predictors of meniscus function: Basic science to clinical translation. *J Orthop Res*, 38: 937–945.  
<https://doi.org/10.1002/jor.24552>
120. Mononen ME, Jurvelin JS, Korhonen RK, 2013, Effects of radial tears and partial meniscectomy of lateral meniscus on the knee joint mechanics during the stance phase of the gait cycle--a 3D finite element study. *J Orthop Res*, 31: 1208–1217.  
<https://doi.org/10.1002/jor.22358>
121. Halonen KS, Mononen ME, Jurvelin JS, *et al.*, 2014, Deformation of articular cartilage during static loading of a knee joint--experimental and finite element analysis. *J Biomech*, 47: 2467–2474.  
<https://doi.org/10.1016/j.jbiomech.2014.04.013>
122. Khoshgoftar M, Torzilli PA, Maher SA, 2018, Influence of the pericellular and extracellular matrix structural properties on chondrocyte mechanics. *J Orthop Res*, 36: 721–729.  
<https://doi.org/10.1002/jor.23774>
123. Yang N, Nayeb-Hashemi H, Canavan PK, 2009, The combined effect of frontal plane tibiofemoral knee angle and meniscectomy on the cartilage contact stresses and strains. *Ann Biomed Eng*, 37: 2360–2372.  
<https://doi.org/10.1007/s10439-009-9781-3>
124. Peña E, Calvo B, Martínez MA, *et al.*, 2005, Finite element analysis of the effect of meniscal tears and meniscectomies on human knee biomechanics. *Clin Biomech (Bristol, Avon)*, 20: 498–507.  
<https://doi.org/10.1016/j.clinbiomech.2005.01.009>
125. Scotti C, Hirschmann MT, Antinolfi P, *et al.*, 2013, Meniscus repair and regeneration: Review on current methods and research potential. *Eur Cell Mater*, 26: 150–170.  
<https://doi.org/10.22203/ecm.v026a11>
126. Zhang ZZ, Chen YR, Wang SJ, *et al.*, 2019, Orchestrated biomechanical, structural, and biochemical stimuli for engineering anisotropic meniscus. *Sci Transl Med*, 11: eaa0750.  
<https://doi.org/10.1126/scitranslmed.aao0750>
127. Longobardi L, O'Rear L, Aakula S, *et al.*, 2006, Effect of IGF-I in the chondrogenesis of bone marrow mesenchymal stem cells in the presence or absence of TGF-beta signaling. *J Bone Miner Res*, 21: 626–636.  
<https://doi.org/10.1359/jbmr.051213>
128. Worster AA, Nixon AJ, Brower-Toland BD, *et al.*, 2000, Effect of transforming growth factor beta1 on chondrogenic differentiation of cultured equine mesenchymal stem cells. *Am J Vet Res*, 61: 1003–1010.  
<https://doi.org/10.2460/ajvr.2000.61.1003>
129. Lee CH, Shah B, Moioli EK, *et al.*, 2015, CTGF directs fibroblast differentiation from human mesenchymal stem/stromal cells and defines connective tissue healing in a rodent injury model. *J Clin Invest*, 125: 3992.  
<https://doi.org/10.1172/jci84508>
130. Furumatsu T, Kanazawa T, Miyake Y, *et al.*, 2012, Mechanical stretch increases Smad3-dependent CCN2 expression in inner meniscus cells. *J Orthop Res*, 30: 1738–1745.  
<https://doi.org/10.1002/jor.22142>
131. Lee CH, Rodeo SA, Fortier LA, *et al.*, 2014, Protein-releasing polymeric scaffolds induce fibrochondrocytic differentiation of endogenous cells for knee meniscus regeneration in sheep. *Sci Transl Med*, 6: 266ra171.  
<https://doi.org/10.1126/scitranslmed.3009696>
132. Nakagawa Y, Fortier LA, Mao JJ, *et al.*, 2019, Long-term evaluation of meniscal tissue formation in 3-dimensional-printed scaffolds with sequential release of connective tissue growth factor and TGF- $\beta$ 3 in an ovine model. *Am J Sports Med*, 47: 2596–25607.  
<https://doi.org/10.1177/0363546519865513>